



A 3-D Magnetic Analysis of a Stirling Convertor Linear Alternator Under Load

Steven M. Geng and Gene E. Schwarze
Glenn Research Center, Cleveland, Ohio

Janis M. Niedra
QSS Group, Inc., Brook Park, Ohio

Timothy F. Regan
Sest, Inc., Middleburg Heights, Ohio

The NASA STI Program Office . . . in Profile

Since its founding, NASA has been dedicated to the advancement of aeronautics and space science. The NASA Scientific and Technical Information (STI) Program Office plays a key part in helping NASA maintain this important role.

The NASA STI Program Office is operated by Langley Research Center, the Lead Center for NASA's scientific and technical information. The NASA STI Program Office provides access to the NASA STI Database, the largest collection of aeronautical and space science STI in the world. The Program Office is also NASA's institutional mechanism for disseminating the results of its research and development activities. These results are published by NASA in the NASA STI Report Series, which includes the following report types:

- **TECHNICAL PUBLICATION.** Reports of completed research or a major significant phase of research that present the results of NASA programs and include extensive data or theoretical analysis. Includes compilations of significant scientific and technical data and information deemed to be of continuing reference value. NASA's counterpart of peer-reviewed formal professional papers but has less stringent limitations on manuscript length and extent of graphic presentations.
- **TECHNICAL MEMORANDUM.** Scientific and technical findings that are preliminary or of specialized interest, e.g., quick release reports, working papers, and bibliographies that contain minimal annotation. Does not contain extensive analysis.
- **CONTRACTOR REPORT.** Scientific and technical findings by NASA-sponsored contractors and grantees.

- **CONFERENCE PUBLICATION.** Collected papers from scientific and technical conferences, symposia, seminars, or other meetings sponsored or cosponsored by NASA.
- **SPECIAL PUBLICATION.** Scientific, technical, or historical information from NASA programs, projects, and missions, often concerned with subjects having substantial public interest.
- **TECHNICAL TRANSLATION.** English-language translations of foreign scientific and technical material pertinent to NASA's mission.

Specialized services that complement the STI Program Office's diverse offerings include creating custom thesauri, building customized data bases, organizing and publishing research results . . . even providing videos.

For more information about the NASA STI Program Office, see the following:

- Access the NASA STI Program Home Page at <http://www.sti.nasa.gov>
- E-mail your question via the Internet to help@sti.nasa.gov
- Fax your question to the NASA Access Help Desk at 301-621-0134
- Telephone the NASA Access Help Desk at 301-621-0390
- Write to:
NASA Access Help Desk
NASA Center for Aerospace Information
7121 Standard Drive
Hanover, MD 21076



A 3-D Magnetic Analysis of a Stirling Convertor Linear Alternator Under Load

Steven M. Geng and Gene E. Schwarze
Glenn Research Center, Cleveland, Ohio

Janis M. Niedra
QSS Group, Inc., Brook Park, Ohio

Timothy F. Regan
Sest, Inc., Middleburg Heights, Ohio

Prepared for the
36th Intersociety Energy Conversion Engineering Conference
cosponsored by the ASME, IEEE, AIChE, ANS, SAE, and AIAA
Savannah, Georgia, July 29–August 2, 2001

National Aeronautics and
Space Administration

Glenn Research Center

Acknowledgments

The authors wish to acknowledge the Stirling Technology Company for providing hardware information and data relative to the DOE/STC Technology Demonstration Converter.

This report contains preliminary findings, subject to revision as analysis proceeds.

Trade names or manufacturers' names are used in this report for identification only. This usage does not constitute an official endorsement, either expressed or implied, by the National Aeronautics and Space Administration.

Available from

NASA Center for Aerospace Information
7121 Standard Drive
Hanover, MD 21076

National Technical Information Service
5285 Port Royal Road
Springfield, VA 22100

Available electronically at <http://gltrs.grc.nasa.gov/GLTRS>

IECEC2001–CT–34

A 3-D MAGNETIC ANALYSIS OF A STIRLING CONVERTOR LINEAR ALTERNATOR UNDER LOAD

Steven M. Geng and Gene E. Schwarze
Glenn Research Center, Cleveland, Ohio

Janis M. Niedra
QSS Group, Inc., Brook Park, Ohio

Timothy F. Regan
Sest, Inc., Middleburg Hts., Ohio

ABSTRACT

The NASA Glenn Research Center (GRC), the Department of Energy (DOE), and the Stirling Technology Company (STC) are developing Stirling convertors for Stirling Radioisotope Power Systems (SRPS) to provide electrical power for future NASA deep space missions. STC is developing the 55-We Technology Demonstration Convertor (TDC) under contract to DOE. Of critical importance to the successful development of the Stirling convertor for space power applications is the development of a lightweight and highly efficient linear alternator.

This paper presents a 3-dimensional finite element method (FEM) approach for evaluating Stirling convertor linear alternators. The model extends a magnetostatic analysis previously reported at the 35th Intersociety Energy Conversion Engineering Conference (IECEC) to include the effects of the load current. STC's 55-We linear alternator design was selected to validate the model. Spatial plots of magnetic field strength (H) are presented in the region of the exciting permanent magnets. The margin for permanent magnet demagnetization is calculated at the expected magnet operating temperature for the near earth environment and for various average magnet temperatures. These thermal conditions were selected to represent a worst-case condition for the planned deep space missions. This paper presents plots that identify regions of high H where the potential to alter the magnetic moment of the magnets exists.

INTRODUCTION

NASA GRC, DOE, and STC are developing a Stirling convertor for an advanced radioisotope power system to provide spacecraft on-board electric power for NASA deep space missions. NASA GRC's role includes an in-house project to provide convertor, component, and materials testing and evaluation in support of the overall power system development. As a part of this work, NASA GRC has established an in-house Stirling Research Laboratory for testing, analyzing, and evaluating Stirling machines (Ref [1]). Four 55-We convertors (TDC 5, 6, 7, and 8) have been built by STC for NASA and are currently under test at GRC. A cross-sectional view of the 55-We TDC is shown in Figure 1. For more information on the TDC, see References [2,3,4]. As another part of this work, NASA GRC has been developing Finite Element Analysis (FEA) and Finite Element Method (FEM) tools for performing various linear alternator thermal and electromagnetic analyses, and evaluating design configurations.

A 3-dimensional (3-D) magnetostatic FEM model of STC's 55-We Technology Demonstration Convertor (TDC) linear alternator was developed by Geng et al (Ref [5]) to evaluate the demagnetization fields affecting the alternator magnets. The model, previously reported at the 35th IECEC, was an open-circuit model. The effect of load current flow through the alternator windings was not included in the preliminary analysis. The predicted alternator open-circuit voltage compared well with the experimentally measured value, which tended to verify the accuracy of the model. The model was then

used to perform a preliminary evaluation of the demagnetization fields acting on the magnets. The preliminary evaluation showed that for the assumed magnet material, UGIMAX 37B, and magnet temperature of 75°C, the magnets margin to demagnetization was approximately 70 kA/m. The effect of current flow through the alternator windings was expected to further reduce this margin to demagnetization for the assumed magnet material.

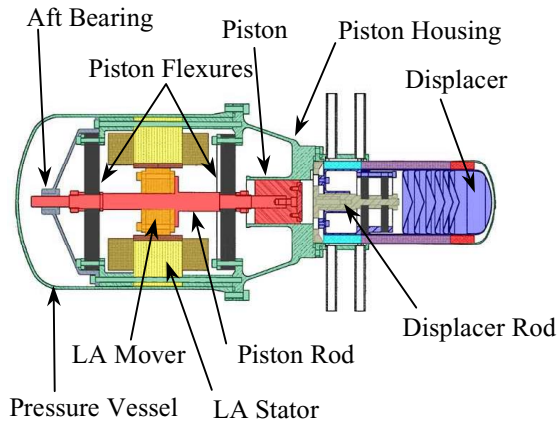


Figure 1 – Cross-section of STC’s 55-We Technology Demonstration Converter (TDC)

The 3-D magnetostatic FEM model of STC’s 55-We TDC linear alternator has been enhanced to include the effect of current flow through the alternator coil windings. The current waveform is now a boundary condition for the magnetostatic model. The linear alternator current and terminal voltage was measured in NASA GRC’s Stirling Research Laboratory for TDC 7 at full design stroke. The measured current was used as a boundary condition in the new linear alternator model. The magnetic properties of the magnets used in the TDCs built for NASA are now in the model and offer a better resistance to demagnetization than the UGIMAX 37B magnets assumed in the original model. The enhanced model was used to generate spatial plots of the magnetic field strength (H) in the region of the permanent magnets. The margin for magnet demagnetization was evaluated at various magnet temperatures.

OBJECTIVE

The objective of this work was to develop an analytical tool that could aid engineers in the design, development, evaluation and understanding of advanced linear alternator designs.

MAGNETOSTATIC/LOAD CURRENT MODEL

A 3-D magnetostatic model of STC’s 55-We linear alternator design was developed using Ansoft’s Maxwell 3-D Field Simulator software (Ref [6]). The magnetostatic model consisted of a quarter section of the linear alternator as described in Ref [5]. The components included the mover laminations, Neodymium-Iron-Boron magnets, stator laminations, and copper coils. Magnetostatic flux solutions were generated for a series of 13 different mover positions over a 1.2 cm mover stroke. For each mover position, the instantaneous current flow through the alternator coil windings was applied as a boundary condition. The linear alternator current was obtained experimentally by GRC for TDC 7. A plot of the experimental data is shown in Figure 2.

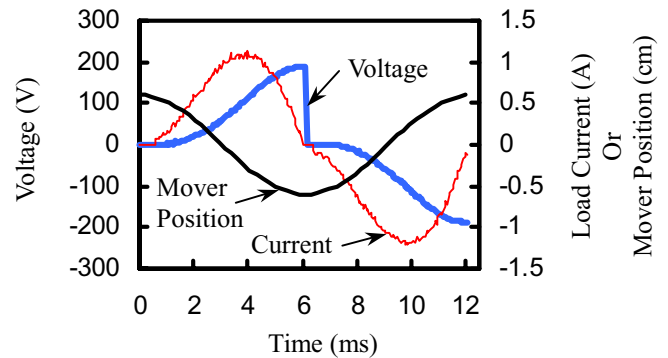


Figure 2 – Experimental Data of Terminal Voltage, Load Current, and Mover Position vs. Time for TDC 7 at Full Stroke

ELECTRO-MAGNETIC ANALYSIS AT ALTERNATOR OPERATING TEMPERATURE UNDER LOAD

A thermal model of STC’s 55-We linear alternator was developed using the ANSYS™ finite element software to evaluate the alternator magnet temperatures for potential space missions. Many assumptions had to be made in preparing the thermal model. For instance, the Stirling convertor pressure vessel was assumed to have an unobstructed view to a radiation sink temperature of -40°C. This sink temperature is a conservative estimate for radiation from a body in space in near earth environment. These thermal conditions were selected to represent a worst-case condition for the planned deep space missions. The emissivity and absorptivity of the radiating surfaces were set to 0.91. Surface conductance between adjacent parts in contact with each other was set to 0.31 W/°C-cm². The efficiency of the alternator was assumed to be 85%. No convection heat transfer was modeled. Assuming a Stirling convertor cold-end temperature of 120°C, the thermal model predicted that the average magnet temperature would be approximately 75°C. At this temperature, the linear alternator

magnets have a remanence B_r of 1.213 Tesla and a coercive force H_c of -900 kA/m.

Figure 3 shows a plot of the magnetic field strength (H) vs. distance along a pair of magnets attached to one stator leg for the mover positioned at the end of stroke. This is a mover position that leaves one of the magnets almost completely exposed. The model predicts that this is the most severe magnet loading over the entire stroke. The plot shows a maximum localized demagnetization field of roughly 725 kA/m on the inside surface of the uncovered magnet. At this magnet temperature, demagnetization can occur for demagnetization fields larger than 884 kA/m. The margin to demagnetization, defined as the difference between H at the knee of the normal induction curve and the maximum localized demagnetization field, is roughly 159 kA/m.

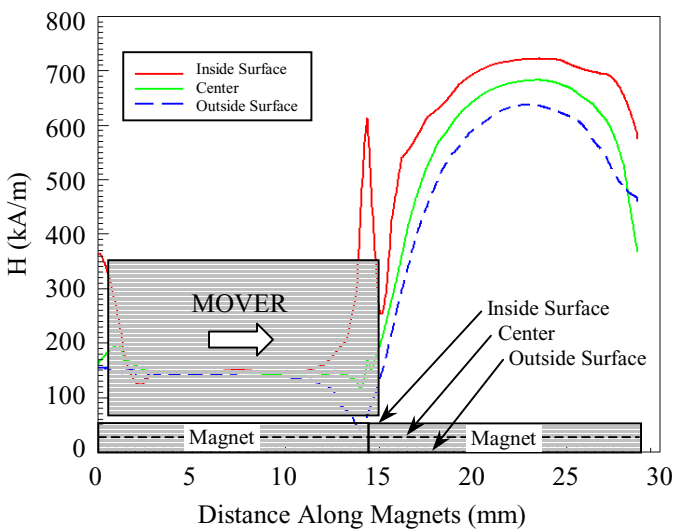


Figure 3 – Magnetic Field Strength $|\vec{H}|$ vs. Distance along Magnets at 75°C; End of Stroke

Figure 4 shows a plot of H vs. distance along the magnets for the mover positioned at mid-stroke. This mover position corresponds to the instant in the cycle of the peak-induced voltage in the coils due to magnet flux. The plot shows that the maximum demagnetization field is about 690 kA/m. The margin to demagnetization is 194 kA/m.

Figure 5 shows a plot of the magnetic field strength (H) vs. distance along the magnets for the mover positioned at maximum current flow. The current lags the induced voltage by approximately 40°. Therefore, the mover position shown in the figure is offset from its mean position. The plot shows a localized maximum demagnetization field of approximately 660 kA/m. The magnet loading is less severe in this case in

comparison with the magnet loading when the mover is at the end of stroke. The fringing fields in the magnet region near the advancing/receding edge of the mover due to the load current appears to be less severe than for the case where the magnet was almost completely exposed. The margin to demagnetization is roughly 224 kA/m.

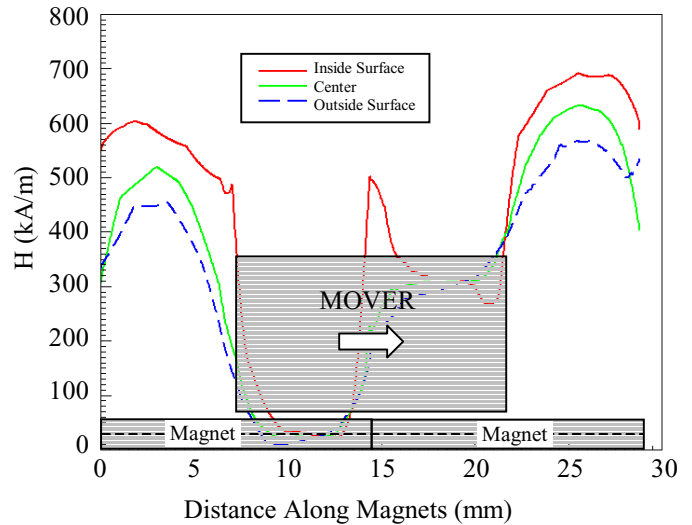


Figure 4 – Magnetic Field Strength $|\vec{H}|$ vs. Distance along Magnets at 75°C; Maximum Induced Voltage (Due to Magnet Flux)

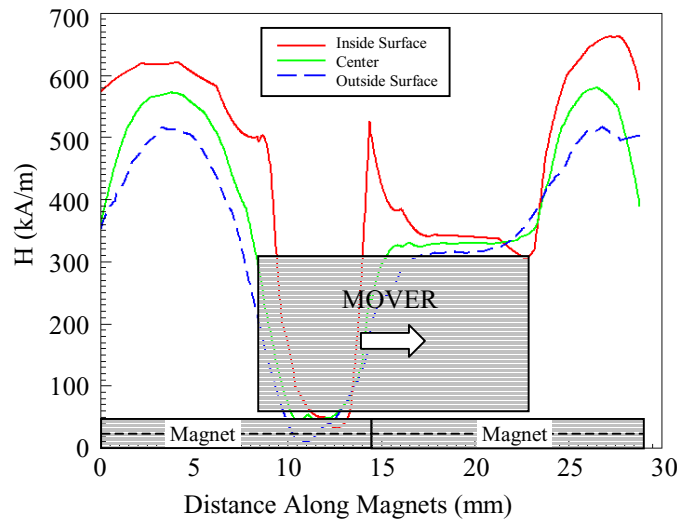


Figure 5 – Magnetic Field Strength $|\vec{H}|$ vs. Distance along Magnets at 75°C; Maximum Load Current

Both Figures 4 and 5 show an interesting characteristic of the linear alternator due to the load current. For the portions of the magnets covered by the mover, the effect of the load current tends to decrease the demagnetization field for one magnet while it tends to increase the demagnetization field for the other magnet over a half-cycle. The effect reverses itself during the second half of the cycle for each magnet. Even though the load current can boost the demagnetization field in the covered portion of the magnet, the demagnetization field for the uncovered portion of the magnet is substantially larger. Figures 4 and 5 also show a small kink in the demagnetization curve for the inside surface of the magnets adjacent to the trailing edge of the mover. This kink might represent a minor fringing effect at this location.

MAGNET LOADING AT VARIOUS TEMPERATURES

The thermal model of STC’s 55-We linear alternator was used to evaluate alternator magnet temperatures for various Stirling convertor cold-end temperatures. For Stirling convertor cold-end temperatures of 100°C and 80°C, the average magnet temperatures were calculated to be approximately 62°C and 53°C, respectively. The linear portion of the magnet’s normal induction curve at each temperature was used in the magnetostatic model of the linear alternator to evaluate the margin to magnet demagnetization as a function of temperature at the most severe magnet load condition (i.e. end of stroke). For a magnet temperature of 62°C, the maximum localized demagnetization field was calculated at 745 kA/m. At this magnet temperature, demagnetization can occur for demagnetization fields larger than 1018 kA/m. The margin to demagnetization is roughly 273 kA/m. For a magnet temperature of 53°C, the maximum localized demagnetization field was calculated at 760 kA/m. At this magnet temperature, demagnetization can occur for demagnetization fields larger than 1108 kA/m. The margin to demagnetization is roughly 348 kA/m.

Figure 6 shows a plot of three variables as a function of magnet temperature. The solid line represents the knee of the normal induction curve based on the magnet manufacturer’s data. If the magnets are subjected to demagnetization fields above this line, some level of magnet demagnetization may occur. The long-dashed line in the figure represents the maximum localized demagnetization field affecting the magnets as predicted by the magnetostatic/load current model. The short-dashed line is the predicted margin to magnet demagnetization for TDCs 5, 6, 7, and 8. This plot shows that the maximum localized demagnetization field for the alternator magnets decreases as temperature increases but at a lower rate than the decrease in the magnet’s ability to resist demagnetization. As a result, the margin to demagnetization decreases as temperature increases. The vertical lines shown on

the plot indicate the magnet temperatures calculated for the various Stirling convertor cold-end temperatures (T_c).

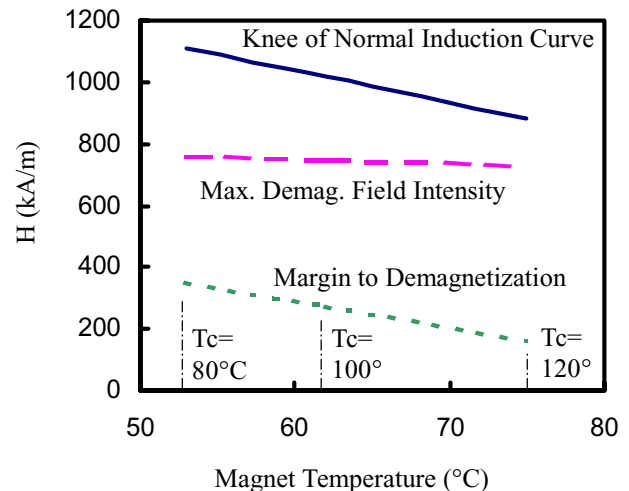


Figure 6 – Sensitivity of Resistance to Demagnetization, Maximum Localized Demagnetization Field Intensity and Margin to Demagnetization as a Function of Temperature

Table 1 summarizes the margin to demagnetization numbers presented in this paper and compares these margins on a percentage basis calculated in two different ways. The column in the Table labeled “Margin Based on Max Localized Demag. Field” computes the percentage by taking the difference between the demagnetization field limit and the maximum localized demagnetization field and dividing by the demagnetization field limit. The column labeled “Margin Based on Demag. Field Avg. Over Magnet Vol.” computes the percentage by taking the difference between the demagnetization field limit and the demagnetization field averaged over the magnet volume and dividing by the demagnetization field limit. The demagnetization field limit represents the knee of the normal induction curve at the given magnet temperature.

Table 1 illustrates that the margin to demagnetization can vary widely depending upon the method chosen to perform the calculation. There is a large difference between the maximum localized demagnetization field and the volume averaged demagnetization field for a given magnet. A magnet that appears safe based on its volume averaged demagnetization field may, in fact, be in jeopardy.

Table 1 – Margin to Magnet Demagnetization

Avg. Magnet Temp. (°C)	Max. Localized Demag. Field (kA/m)	Demag. Field Avg. Over Magnet Volume (kA/m)	Demag. Field Limit (kA/m)	Margin Based On Max. Localized Demag. Field (%)	Margin Based On Demag. Field Avg. Over Magnet Vol. (%)
53	760	550	1108	31	50
62	745	539	1018	27	47
75	725	527	884	18	40

CONCLUSIONS

The results shown by this preliminary 3-D analysis indicate that the highest potential for demagnetization appears to be along the inside surface of the uncovered magnets. The demagnetization field for the uncovered magnet when the mover is at the end of stroke is higher than for when the mover is at the position of maximum induced voltage or maximum load current. The demagnetization field and the magnet’s resistance to demagnetization decrease with increasing temperature; however, the magnet’s resistance to demagnetization decreases at a higher rate. The magnet’s margin to demagnetization decreases as magnet temperature increases as expected. Based on the results presented in this paper, it appears that the 55-We TDCs built for NASA can operate safely at magnet temperatures up to 75°C, provided that no abnormal load conditions occur.

REFERENCES

[1] Thieme, L.G., Schreiber, J.G.: “NASA GRC Technology Development Project for a Stirling Radioisotope Power System,” in Proceedings from 35th Intersociety Energy Conversion Engineering Conference, Las Vegas, Nevada, AIAA-2000-2840, NASA TM-2000-210246, 2000.

[2] Thieme, L.G., Qiu, S., White, M.A.: “Technology Development for a Stirling Radioisotope Power System,” NASA TM-2000-209791, 2000.

[3] White, M.A., Qiu, S., Augenblick, J.E.: “Preliminary Test Results from a Free-Piston Stirling Engine Technology Demonstration Program to Support Advanced Radioisotope Space Power Applications,” in Proceedings from STAIF-00, Space Technology and Applications International Forum-2000, Albuquerque, New Mexico, 2000.

[4] White, M.A., Qiu, S., Augenblick, J.E., Peterson, A., Faultersack, F.: “Status Update of a Free-Piston Stirling Converter For Radioisotope Space Power Systems,” in Proceedings from STAIF-01, Space Technology and Applications International Forum-2001, Albuquerque, New Mexico, 2001.

[5] Geng, S.M., Schwarze, G.E., Niedra, J.M.: “A 3-D Magnetic Analysis of a Linear Alternator for a Stirling Power System,” in Proceedings from 35th Intersociety Energy Conversion Engineering Conference, Las Vegas, Nevada, AIAA-2000-2838, NASA TM-2000-210249, 2000.

[6] Ansoft’s Maxwell 3-D Field Simulator, see World Wide Web page: www.ansoft.com

REPORT DOCUMENTATION PAGE			<i>Form Approved</i> <i>OMB No. 0704-0188</i>	
Public reporting burden for this collection of information is estimated to average 1 hour per response, including the time for reviewing instructions, searching existing data sources, gathering and maintaining the data needed, and completing and reviewing the collection of information. Send comments regarding this burden estimate or any other aspect of this collection of information, including suggestions for reducing this burden, to Washington Headquarters Services, Directorate for Information Operations and Reports, 1215 Jefferson Davis Highway, Suite 1204, Arlington, VA 22202-4302, and to the Office of Management and Budget, Paperwork Reduction Project (0704-0188), Washington, DC 20503.				
1. AGENCY USE ONLY (<i>Leave blank</i>)	2. REPORT DATE July 2001	3. REPORT TYPE AND DATES COVERED Technical Memorandum		
4. TITLE AND SUBTITLE A 3-D Magnetic Analysis of a Stirling Convertor Linear Alternator Under Load			5. FUNDING NUMBERS WU-783-82-00-00	
6. AUTHOR(S) Steven M. Geng, Gene E. Schwarze, Janis M. Niedra, and Timothy F. Regan				
7. PERFORMING ORGANIZATION NAME(S) AND ADDRESS(ES) National Aeronautics and Space Administration John H. Glenn Research Center at Lewis Field Cleveland, Ohio 44135-3191			8. PERFORMING ORGANIZATION REPORT NUMBER E-12928	
9. SPONSORING/MONITORING AGENCY NAME(S) AND ADDRESS(ES) National Aeronautics and Space Administration Washington, DC 20546-0001			10. SPONSORING/MONITORING AGENCY REPORT NUMBER NASA TM-2001-211084 IECEC2001-CT-34	
11. SUPPLEMENTARY NOTES Prepared for the 36th Intersociety Energy Conversion Engineering Conference cosponsored by the ASME, IEEE, AIChE, ANS, SAE, and AIAA, Savannah, Georgia, July 29-August 2, 2001. Steven M. Geng and Gene E. Schwarze, NASA Glenn Research Center; Janis M. Niedra, QSS Group, Inc., 2000 Aerospace Parkway, Brook Park, Ohio 44142; Timothy F. Regan, <i>Sest, Inc.</i> , 18000 Jefferson Park, Suite 104, Middleburg Heights, Ohio 44130. Responsible person, Steven M. Geng, organization code 5490, 216-433-6145.				
12a. DISTRIBUTION/AVAILABILITY STATEMENT Unclassified - Unlimited Subject Category: 20 Available electronically at http://gltrs.grc.nasa.gov/GLTRS This publication is available from the NASA Center for AeroSpace Information, 301-621-0390.			12b. DISTRIBUTION CODE	
13. ABSTRACT (<i>Maximum 200 words</i>) The NASA Glenn Research Center (GRC), the Department of Energy (DOE), and the Stirling Technology Company (STC) are developing Stirling convertors for Stirling Radioisotope Power Systems (SRPS) to provide electrical power for future NASA deep space missions. STC is developing the 55-We Technology Demonstration Convertor (TDC) under contract to DOE. Of critical importance to the successful development of the Stirling convertor for space power applications is the development of a lightweight and highly efficient linear alternator. This paper presents a 3-dimensional finite element method (FEM) approach for evaluating Stirling convertor linear alternators. The model extends a magnetostatic analysis previously reported at the 35th Intersociety Energy Conversion Engineering Conference (IECEC) to include the effects of the load current. STC's 55-We linear alternator design was selected to validate the model. Spatial plots of magnetic field strength (H) are presented in the region of the exciting permanent magnets. The margin for permanent magnet demagnetization is calculated at the expected magnet operating temperature for the near earth environment and for various average magnet temperatures. These thermal conditions were selected to represent a worst-case condition for the planned deep space missions. This paper presents plots that identify regions of high H where the potential to alter the magnetic moment of the magnets exists.				
14. SUBJECT TERMS AC generators; Stirling engines; Free-piston engines			15. NUMBER OF PAGES 11	
			16. PRICE CODE	
17. SECURITY CLASSIFICATION OF REPORT Unclassified	18. SECURITY CLASSIFICATION OF THIS PAGE Unclassified	19. SECURITY CLASSIFICATION OF ABSTRACT Unclassified	20. LIMITATION OF ABSTRACT	

